Published online 1 August 2023 *Nucleic Acids Research, 2023, Vol. 51, No. 15* ***8035–8047***
https://doi.org/10.1093/nar/gkad647

Single-worm long-read sequencing reveals genome diversity in free-living nematodes

Yi-Chien Lee[1,2,3], Huei-Mien Ke[4], Yu-Ching Liu[1], Hsin-Han Lee[1], Min-Chen Wang[5], Yung-Che Tseng[5], Taisei Kikuchi[6] and Isheng Jason Tsai[1,2,*]

[1]Biodiversity Research Center, Academia Sinica, Taipei 115, Taiwan, [2]Biodiversity Program, Taiwan International Graduate Program, Academia Sinica and National Taiwan Normal University, Taipei, Taiwan, [3]Department of Life Science, National Taiwan Normal University, 116 Wenshan, Taipei, Taiwan, [4]Department of Microbiology, Soochow University, Taipei, Taiwan, [5]Marine Research Station (MRS), Institute of Cellular and Organismic Biology, Academia Sinica, 262 I-Lan County, Taiwan and [6]Department of Integrated Biosciences, Graduate School of Frontier Sciences, The University of Tokyo, Chiba 277-8562, Japan

Received April 19, 2023; Revised July 10, 2023; Editorial Decision July 11, 2023; Accepted July 21, 2023

ABSTRACT

Obtaining sufficient genetic material from a limited biological source is currently the primary operational bottleneck in studies investigating biodiversity and genome evolution. In this study, we employed multiple displacement amplification (MDA) and Smart-seq2 to amplify nanograms of genomic DNA and mRNA, respectively, from individual *Caenorhabditis elegans*. Although reduced genome coverage was observed in repetitive regions, we produced assemblies covering 98% of the reference genome using long-read sequences generated with Oxford Nanopore Technologies (ONT). Annotation with the sequenced transcriptome coupled with the available assembly revealed that gene predictions were more accurate, complete and contained far fewer false positives than *de novo* transcriptome assembly approaches. We sampled and sequenced the genomes and transcriptomes of 13 nematodes from early-branching species in Chromadoria, Dorylaimia and Enoplia. The basal Chromadoria and Enoplia species had larger genome sizes, ranging from 136.6 to 738.8 Mb, compared with those in the other clades. Nine mitogenomes were fully assembled, and displayed a complete lack of synteny to other species. Phylogenomic analyses based on the new annotations revealed strong support for Enoplia as sister to the rest of Nematoda. Our result demonstrates the robustness of MDA in combination with ONT, paving the way for the study of genome diversity in the phylum Nematoda and beyond.

GRAPHICAL ABSTRACT

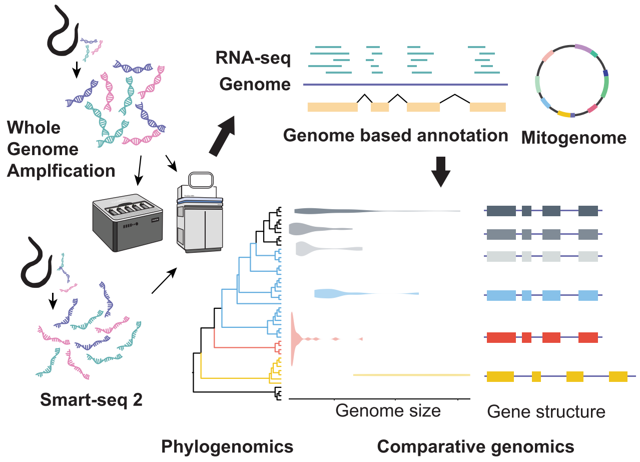

INTRODUCTION

A genome reference is a prerequisite for a complete understanding of the biology and evolution of a species. Advances in long-read sequencing, together with increasing affordable costs (1), have paved the way for the ambition to study and generate genomes for the entire group of species, including every bird, vertebrate, insect or eukaryote on Earth (2–5). However, the major challenge remains obtaining high-quality DNA and RNA from the majority of organisms across the tree of life (6). Such requirements are challenging to meet in microscopic organisms that cannot be cultured, leading to sampling bias and loss of their biological information on genetic and evolutionary studies (7–9). Recent advances in whole-genome amplification (WGA) have enabled single cells or limited samples to generate sufficient DNA for sequencing (10,11), and have been applied

[*]To whom correspondence should be addressed. Tel: +886 2 2787 2270; Fax: +886 2 2789 9624; Email: ijtsai@gate.sinica.edu.tw

to eukaryotic microorganisms, including fungi (9,12), marine phytoplankton (13) and parasitic nematodes (14,15), for genomic and population genetic studies (9,16).

This study investigated the feasibility of WGA combined with long-read sequencing for nematodes, which are the most abundant metazoans on Earth. More than 40 million to 81.6 million nematode species are estimated to exist, but only ∼25,000 species have been described so far (17,18). The Nematoda phylum has been classified on the basis of 18S rRNA into three lineages and five major clades: Dorylaimia (clade I), Enoplia (clade II) and Chromadoria (clade III–V). Chromadoria further include Spirurina (clade III), Tylenchina (clade IV) and Rhabditina (clade V) as well as early derived lineages including Araeolaimida, Chromadorida, Desmodorida, Monhysterida and Plectida (19–21). The roundworm *Caenorhabditis elegans* was the first animal to have its genome sequenced, with a size of 100.3 Mb. Since then, >200 nematode genomes and mitogenomes have been published (22,23). Of these, ∼72% are mainly terrestrial parasites belonging in Dorylaimia, Spirurina and Tylenchina because of their importance in plant crops and animal health. The remaining species are terrestrial free-living nematodes in Rhabditina (17,24,25). In contrast, only one genome of a marine nematode, *Litoditis marina* (26), is available, despite the fact that marine nematodes comprise half of all recorded nematodes and play a crucial role in benthic communities as decomposers, predators, food sources and bioindicators (27). Only a few marine nematode species belonging to Monhysterida and Rhabditida (26,28) can be cultured. Thus, obtaining enough genomic DNA for sequencing is challenging for most of these species, making them potential candidates for the WGA techniques.

The Enoplia clade and the early derived Chromadoria lineage (19), found primarily in marine habitats, currently lack genomic data and have several important implications. Of particular interest is the phylogenetic relationship of basal nematodes, which remains unresolved due to insufficient sampling and limited resolution of 18S rRNA (20). Resolving the phylogenetic relationship of nematodes can help to understand the genomic basis of nematode diversity and the processes of evolution from free-living to a parasitic lifestyle (21,29). Increased sampling of marine nematodes and phylogenomic analyses based on mitogenomes or *de novo* transcriptomes have shown improved resolution of Enoplia sister to the rest of the Nematoda (19,22,30–32). Gene models predicted from genome assemblies will further confirm these findings.

Here, we have developed an assembly and annotation workflow capable of generating transcriptome and long genome sequences from single nematodes. We quantified the coverage biases in the amplified sequences, produced assemblies and assessed the accuracy of the annotations using this workflow on *C. elegans* compared with those generated *de novo* without a genome available. The finalized workflow was applied to 13 free-living marine nematodes isolated from the Taiwanese coasts. Despite obtaining lower genome coverage in these nematodes, phylogenomic analyses were performed using a total of 331,551 newly annotated genes to resolve the positions of basal clades in the Nematoda phylum. Comparisons of the genomes and complete mitogenomes of these nematodes revealed remarkable variation in genome features not observed in more studied clades and shed light on the early evolution of nematodes.

MATERIALS AND METHODS

Single-worm DNA extraction

Caenorhabditis elegans strain N2 was grown at 22°C on nematode growth medium (NGM) plates with *Escherichia coli* strain OP50, and *Aphelenchoides besseyi* APVT strain was grown at 22°C on potato dextrose agar (PDA) plates with *Alternaria citri*. Worms were either washed with M9 buffer from NGM plates and pelleted in a 15 ml centrifuge tube, or washed with the same M9 buffer three times and starved in M9 buffer that included 1% antibiotic–antimycotic (Thermo Fisher Scientific, MA, USA, 15240062) in a 15 ml centrifuge tube for 24 hr. A total of 13 nematode species (*Epsilonema* sp., *Enoplolaimus lenunculus*, *Linhomoeus* sp., *Microlaimidae* sp., *Mesodorylaimus* sp., *Paralinhomoeus* sp., *Ptycholaimellus* sp., *Trileptium ribeirensis*, *Sabatieria punctata*, *Rhynchonemsa* sp., *Theristus* sp., *Trissonchulus latispiculum* and *Trissonchulus* sp.) were collected in Taiwan between November 2020 and May 2022 (Supplementary Table S1). The sampling locations include seashores around Taiwan and 15–18 m depth sea bottom around Guishan island. Single individuals were isolated and washed with 10% bleach for 10 s and transferred into 200 μl polymerase chain reaction (PCR) tubes containing lysis buffer [8 μl of direct PCR lysis reagent (Viagen, #102-T), 1 μl of 5 mg/ml proteinase K and 1 μl of 200 mM dithiothreitol (DTT)] and incubated in 65°C for 20 min and 95°C for 5 min. The DNA concentrations were quantified with the Qubit dsDNA HS Assay Kit (Thermo Fisher Scientific, 2339927) following the manufacturer's instructions.

Whole-genome amplification

Various sources of extracted genomic DNA (gDNA) were used for amplification (Supplementary Figure S1). (i) Whole worm: one worm or 10 adult worms were cut into pieces with a 22-gauge needle in a 200 μl PCR tube. In one amplification instance, a single whole worm was prepared with 5% dimethylsulfoxide (DMSO) added in polymerase mix. Genomic DNA extraction and amplification were performed with the Qiagen REPLI-g Kit (150023,150043,150343, Qiagen, German). (ii) Purified DNA: single-worm DNA extraction with lysis buffer [8 μl of direct PCR lysis reagent (Viagen, #102-T), 1 μl of 5 mg/ml proteinase K, 1 μl of 200 mM DTT) and incubated in 65°C for 20 min and 95°C for 5 min. The samples were further purified using a 1:1 v/v ratio of sample to Ampure XP beads (A63882, Beckman Coulter, USA) and eluted in 10 μl of elution buffer. The MDA step was performed with the REPLI-g Kit (150023, Qiagen) following the manufacturer's instructions. A detailed protocol is available at protocols.io.

Genomic DNA library preparation, sequencing and assembly

The amplified genomic DNA was sent to Biotools Co., Ltd (New Taipei City, Taiwan) for library preparation and sequencing of Illumina 150 bp paired-end reads on a Novaseq 6000 sequencer. Genome sizes were estimated from Illumina reads using Jellyfish (ver. 2.3.0; -m 21) (33) and GenomeScope 2.0 (34). For Oxford Nanopore sequencing, two digestion times were initially tested on *C. elegans* using 1.5 μg of amplified gDNA from one or 10 adult worms. Templates were digested with T7 endonuclease I (M0302L, NEB, USA) for either 15 min, as recommended for sequencing whole-genome-amplified *E. coli* gDNA on the ONT community website (SQK-LSK109; ver. WAL_9070_v109_revN_14Aug2019) or 30 min. For the other nematodes, 3 μg of amplified templates were digested with T7 endonuclease I for 30 min and subjected to library preparation according to the manufacturer's instructions. Oxford Nanopore libraries were prepared according to SQK-LSK109 and SQK-LSK110 protocols, and a flowcell was sequenced in each species on a GridION instrument. Basecalling of Nanopore raw signals was performed using Guppy [ver. 6.1.2; with a super-accuracy (sup) model] into a total 224.5 Gb of raw reads at least 1 kb or longer. A summary of the sequencing data is shown in Supplementary Table S2.

We identified artificial palindromic sequences, described as reads that map to the reverse complement version of themselves either from the end or at least 30% within the middle of the reads, through Minimap2 alignments (version 2.1; -x ava-ont) (35). These palindromic sequences were extracted from raw reads and corrected by dividing the read from the midpoint of the alignment. This process was performed in two iterations using custom Perl scripts (available at https://zenodo.org/record/8144614), as a sequence may encompass multiple copies of the original fragment (36). Supplementary Table S3 provides a summary of the corrected sequencing data.

The Flye (ver. 2.9.1; option: –nano-hq) assembler (37) was used to assemble the raw ONT reads, which were then polished by four iterations of Racon (38) (ver. 1.4.11), followed by Medaka (ver. 1.2.0; option: -m r941_min_sup_g507 or r103_sup_g507; https://github.com/nanoporetech/medaka). The consensus sequences were further corrected with Illumina reads using NextPolish (39) (ver. 1.4.0), and haplotigs were removed using HaploMerger2 (40) (ver. 20180603). Contigs with non-nematode origins were excluded (see below for details). Genome completeness was assessed using the nematode dataset of BUSCO (41) (ver. 5.1.2). Assemblies were mapped to the reference genome with minimap2 (option: -ax asm5) (35), and genome coverage was calculated using BEDtools (ver. 2.26.0) (42). Raw Illumina reads were assembled using the Spades assembler (ver. v3.14.1; option: spades_sc) (43). The mitochondrial genome was assembled separately by aligning Oxford Nanopore reads to a mitochondrial protein-coding gene of 52 nematode species listed in Supplementary Table S4 using DIAMOND (44), following the approach described in (45). Circularized assemblies were further annotated and manually curated using two versions of Mitos (ver. 1.0.5) and Mitos2 (ver. 2.1.0) (46). The quality and completeness of the various *C. elegans* genome assemblies were compared using WebQUAST (utilizing the *C. elegans* WBcel235 genome with default option) (47) and BUSCO scores (ver. v5.1.2; option: eukaryota_odb10) (41).

Single-worm RNA transcriptome sequencing and assembly

The Smart-seq 2 protocol (48) was used to extract and amplify RNA from single adult worms. The resulting cDNA was sent to Biotools Co., Ltd (New Taipei City, Taiwan) for library preparation using the NEBNext® DNA Library Prep Kit (NEB, USA, 20015828, 20015829), and sequenced for 150 bp paired-ends on an Illumina HiSeq 2500 sequencer. Individual sample statistics are provided in Supplementary Table S2. We utilized FastQC (ver. v0.11.9; https://www.bioinformatics.babraham.ac.uk/projects/fastqc/) to identify over-represented sequences, which we then matched against the NCBI nt database. If the matched sequences were predominantly associated with rRNA sequences, they were incorporated into the adaptor library. Sequencing reads were quality and adaptor trimmed using Trimmomatic (ver. 0.39) (49). On average, 30% of the reads in each sample were identified as rRNA sequences and, after removal, 21–86% of the reads remained. *De novo* transcriptome assemblies were generated using the Spades assembler (ver. v3.14.1; option: -k = 55,77) (43). The best protein-coding predictions from *de novo* assembled transcripts were produced using Transdecoder (ver. 5.5.0; https://github.com/TransDecoder/TransDecoder) integrating homology information from the UniProt database (Release version 2021_03).

Genome annotation

Repetitive elements were identified using RepeatModeler (ver. 2.1) (50), TransposonPSI (ver. 1.0.0; https://github.com/NBISweden/TransposonPSI) and USEARCH (ver. 11.0) (51) based on the protocol by Berriman *et al.* (https://protocolexchange.researchsquare.com/article/nprot-6761/v1). Repetitive DNA sequences were identified and masked using Repeatmasker (ver. 4.1.2; http://www.repeatmasker.org). Proportions of repeat content along the non-overlapped 100 kb window were calculated using BEDTools (ver. 2.26.0) (42).

The proteomes of 11 representative nematodes were obtained from WormBase WBPS18 (52) and are listed in Supplementary Table S5. Single-worm transcriptome reads were mapped to the corresponding genome assemblies using STAR (ver. 2.7.7a) (53). The gene models were predicted using BRAKER2 (ver. 2.1.6; option: –etpmode) (54) with proteomes and RNA-seq mappings as evidence hints. Transcript predictions were mapped to the reference genome using Minimap2 (-ax splice) (35), converted to gff format and compared against the reference proteome using Gffcompare (ver. v0.11.2) (55).

Decontamination

To identify contigs of non-nematode origin, we used a combination of three methods. First, we employed Kraken2 (ver. 2.1.2) (56) to determine the kingdom and phylum of scaffolds based on k-mers. We rebuilt a custom Kraken2 database to include: Archaea, Bacteria, Nematoda, Eukaryota (Annelida, Arthropoda, Cnidaria, Chordata, Porifera, Placozoa and Platyhelminthes), outgroup (human), viruses and undefined. A list of species in the reconstructed database is provided in Supplementary Table S6. The BRAKER2 models were searched against the NCBI nr database using BLAST to assign phylum categories, such as Nematoda, Bacteria, Eukaryota, Eukaryotea-undef, Candidatus, Fungi, Planta, Viruses, Algae, Archaea and Unclassified. Third, we aligned RNA-seq reads for each species to the corresponding genome assemblies using STAR and calculated the RNA-seq mapping rate of each scaffold using BEDTools (ver. 2.26.0) (42). We excluded scaffolds assigned to bacteria by Kraken2 and those with genes that contained ≥90% bacterial proteins. For scaffolds that could not be identified by Kraken2 or the NCBI nr database, we removed those with <1,000 RNA-seq mapped reads.

Phylogenomics of nematodes

Protein datasets from 13 representative nematodes were download from WormBase WBPS18 (52) (Supplementary Table S7). We also downloaded the assembled transcripts of nine nematode species, an outgroup Nematodmorpha from Smythe *et al.* (19) and 19 nematode species from Ahmed *et al.* (32) (Supplementary Table S7). Species with BUSCO completeness > 20% were included in the phylogenomics analyses. Orthogroups (OGs) were identified using OrthoFinder (57). Sequences in OGs were aligned using MAFFT (ver. 7.515) (58). Gene trees were inferred from OGs containing >15% of the species and alignment length longer than 200 bp using VeryFastTree (ver. 4.0) (59), and a species tree was inferred from all OG gene trees using ASTRAL-Pro (60). Two sets of data were used to construct the nematode species phylogeny: (i) the 13 proteomes of nematode species downloaded from WormBase, 13 free-living nematodes sequenced in this study and outgroup *Priapulus cauatus,* comprising a total of 27 species with 46,158 OGs (Supplementary Table S7)*;* and (ii) 27 species with genomes from the first dataset, *de novo* transcriptomes of five species (four nematodes and one *Gordius* sp.) from Smythe *et al.* (19) and 13 species from Ahmed *et al*. (32), *Drosophilamelanogaster* and *Paramacrobiotus metropolitanus*, comprising a total of 47 species with 58,381 OGs. Gene trees from 9,343 and 7,898 OGs were chosen and used to infer the species tree in the first and second dataset, respectively.

RESULTS

Whole-genome amplification facilitates sufficient DNA for long-read sequencing from single nematodes

To study the genome diversity of free-living nematodes, we isolated nematodes from a variety of marine environments in Taiwan and extracted the gDNA from individual adults across 11 taxa, including the Enoplia clade, for which genome sequences are currently unavailable (Supplementary Table S1). Highlighting the challenge of obtaining sufficient gDNA for long-read sequencing across the Nematoda phylum, we found that yields ranged from 1.5 to 3.8 ng for individual adults and were not associated with worm size (Kendall's $\tau = 0.2$, $P = 0.33$; Supplementary Table S8). To mitigate this problem, we used MDA to amplify whole genomes from individual nematodes, yielding 6.2–51.5 μg, corresponding to ∼4,700× and 22,000× amplification using REPLI-g mini kits and REPLI-g midi or sc kits, respectively (Supplementary Table S2). To assess potential amplification bias, we first sequenced the genome of the model nematode *C. elegans* N2. A total of 35 μg of gDNA was obtained after MDA from an initial 1.56 ng, and sequencing using an ONT 9.4.1 flow cell yielded 7.36 Gb with an N50 of 7.74 kb, corresponding to 73.6× depth of coverage (61) (Supplementary Table S2).

Whole-genome amplification disparity in repetitive regions

MDA suffers from several challenges, the most important of which is highly uneven amplification (62,63). This issue can lead to incomplete genome assembly and reduced coverage in certain genome regions, and affect analyses such as copy number variants (63,64). We aligned the amplified and published unamplified ONT reads (65) against the *C. elegans* genome, and the former clearly displayed an uneven depth of coverage, with 19.2% of the non-overlapping 100 kb window showing less than half of the genome-wide median (Figure 1A). Sequencing of the amplified DNA using Illumina short reads also exhibited similar patterns, suggesting that the MDA rather than the sequencing platforms was causing the bias (Supplementary Figure S2A). The intra-chromosomal heterogeneity of the enriched repeats present in the nematode autosome ends was clearly associated with this unevenness. In the six *C. elegans* chromosomes, the end region contains a significantly higher number of repeat sequences ($P \leq 0.001$, Wilcoxon rank sum test) and a lower read coverage ($P \leq 0.001$, Wilcoxon rank sum test; Supplementary Figure S2B, 2C) compared with the center region. However, in the X chromosome, the read coverage is more balanced due to the lower percentage of repeats in the end region (median of repeats 16–21% versus 15–39% in autosomes; Supplementary Figure S2D).

We calculated the proportions of 17 genomic features in 100 kb non-overlapping windows and found that the presence of rolling-circle transposable elements (RC/Helitron) contributed least to sequence coverage ($R^2 = 0.36$, $P < 22e\text{-}16$, Pearson test), followed by unclassified repeats, DNA transposable elements and satellites (Supplementary Figure S3), suggesting that the reduced coverage displayed at autosome ends was mainly due to enriched repeats (61). Within repeat classes, other repeats were the primary repeat class affecting coverage (Figure 1B; Supplementary Figure S4). Of 6,332 rolling-circle transposable element regions totaling 1,409,947 bp, on average there is a 36.7% reduction of coverage compared with the genome median (68× versus 25×; Supplementary Figure S4). The coverage of amplified data on the gene, retrotransposon and other small repeats was significantly lower than of unamplified data (Figure 1B). Finally, we determined 0.49 Mb that were not sequenced at all, ranging from 2 to 40,137 bp. Of these, 17% were repeats and 80 (0.3%) genes were affected. Ten genes located at the ends of chromosomes III, IV, V and X were not completely sequenced (Figure 1C). At the exon

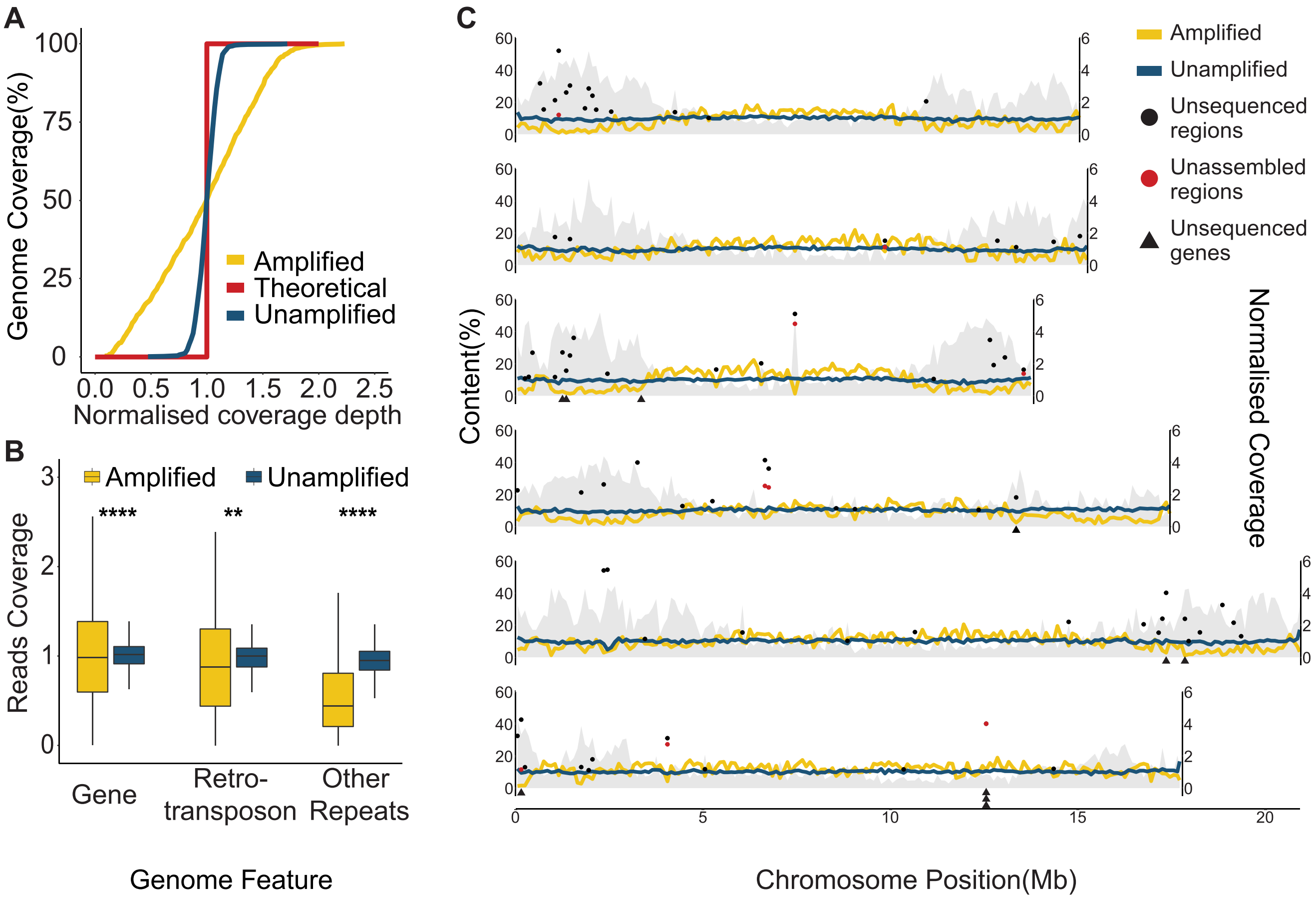

Figure 1. Sequencing coverage of *C. elegans* genomic DNA. (**A**) Cumulative genome coverage versus the genome-wide median. The red line indicates the theoretical coverage of unbiased coverage. More deviation away from this line suggests less uniformity across the genome. (**B**) Normalized read coverage on genes and repeats. Repeats were categorized into two groups: retrotransposons and other repeats. Retrotransposons include long interspersed nuclear elements (LINEs), short interspersed nuclear elements (SINEs) and long terminal repeats (LTRs). DNA transposons, RC Helitron, rRNA, snRNA, tRNA, satellite, simple repeat and unknown repeats were together labeled as other repeats. ***P*≤ 0.01, *****P*≤ 0.0001. (**C**) Lines represent normalized read coverage of amplified and unamplified data. The black and red dots represent the top 10% of regions (11.1–44.8 kbp and 10.1–54.5 kbp) that were not sequenced and not assembled. The triangles represent the position of genes that were not sequenced at all. The shaded area indicates the proportions of repeats along the chromosomes.

level, 0.09% were also affected, including 96 unsequenced CDS.

Due to differences in repeat content between species, we sought to evaluate the impact of MDA by analyzing the amplified reads from the genome of the plant-parasitic nematode *A. besseyi*, which has a smaller genome (44.7 Mb) and lower repeat content (5.38%) compared with other nematodes (66). A similar but less pronounced pattern of uneven coverage was observed in this nematode compared with *C. elegans* (Supplementary Figure S5A). In the *A. besseyi* chromosomes, the chromosome end also contains a significantly higher percentage of repeat sequences and lower read coverage (*P*≤ 0.001, Wilcoxon rank sum test; Supplementary Figure S5B, C). While we observed reduced coverage in repeat regions, we were able to capture most of the genome, with only 0.06% (29,230 bp) of the genome not sequenced, with missing regions ranging from 1 to 2,540 bp and affecting only six repeats and four genes. Taken together, these observations suggest that the MDA approach is a robust approach for capturing most of the genome, although additional sequencing may be required to rescue repetitive regions in some species.

Presence of palindromic sequences after whole-genome amplification

An additional challenge arising from the MDA process is the unintended creation of chimeric fragments which hamper downstream analysis (67). These fragments include inverted repeat sequences, commonly referred to as palindromes, which are the result of continuous amplification of branched DNA produced during the displacement process (36,68). We identified 8.8–30.9% of *C. elegans* samples as palindromes (Supplementary Figure S6). By dividing these sequences from the center of the palindrome (see the Materials and Methods), their prevalence was down to 1.2–5.7% (Supplementary Figure S6). This procedure led to an averaged sequence N50 and number of long sequence (designated as ≥50 kb) reduction by 1.3 kb and 57.6% (Supplementary Table S2 and S3), respectively, indicating that numerous long sequences in the dataset were chimeras. The genome coverage of the palindrome reads paralleled that of non-palindrome reads (Supplementary Figure S7), presumably showing that the chimera generation process occurred randomly.

Longer T7 endonuclease digestion time increase ONT sequencing performance

To enhance the yield and minimize the bias of sequencing amplified samples, we attempted to optimise different stages of the workflow (Supplementary Figure S1). One of the challenges was that the branching templates generated by MDA were unsuitable for Oxford Nanopore sequencing as they can block sequencing pores and reduce sequencing yield (69). T7 endonuclease I was used in the existing protocol to generate linear templates by cutting the junction of the branching template. We found that the digestion time of T7 endonuclease I affected the drop-out rate of sequencing pores and sequencing output (Supplementary Figure 8A) (70). A longer digestion time (30 versus 15 min) improved the sequencing performance by reducing the dropping rate of sequencing pores and increasing the sequencing yield (Supplementary Figure S8B, C). In addition, we tried three other approaches to address the influence of repeats that reduce amplification efficiency (Supplementary Figure S1), but no improvement was observed (Supplementary Figure S2A), indicating that uneven coverage is related more to the polymerase efficiency in amplifying repeats.

Complete genome assemblies from amplified sequences

To evaluate the feasibility of generating assemblies from amplified sequences, we generated genome assemblies of *C. elegans* based on different data types and sources (Supplementary Table S9). On average, 112.5× Illumina and 32.6–88.6× ONT reads were used; the initial assemblies produced under the default options yielded 77.7–115.0 Mb and the recently updated size of 102 Mb (71), suggesting that the biased genome coverage in the amplified reads remains a challenge in the assembly process. Correcting the palindromes in the amplified samples led to more accurate assemblies (Supplementary Table S10), which will be used for all downstream analyses. The final assemblies were produced using the meta option of the Flye assembler, with haplotigs removed, screened for contamination and polished using Illumina reads (see the Materials and Methods), resulting in more similar genome sizes (97.3–98.4 Mb, Supplementary Table S9). Compared with the assembly from unamplified long sequences (65), the N50 of the genome-amplified assembly is 91% shorter than that of the unamplified data, presumably due to the shorter ONT sequence length achieved by MDA (Table 1).

We assessed the completeness of the *de novo* assemblies of single and 10 pooled nematode(s) by first aligning their contigs back to the reference. The unamplified data covered 100.0% of the reference genome, compared with 97.4% for the single-worm amplified assembly (Table 1). A total of 2.5–4.4 Mb of the reference genome was not covered by the amplified genomes. We benchmarked the completeness of the assemblies using universal single-copy orthologs [BUSCO (41)], which were similar regardless of amplification (Table 1). The unassembled regions coincided with unsequenced or highly repetitive regions which were mostly located on the chromosome ends (Figure 1C). Taken together, the results show that the capability of sequencing the genome of the nematode with only a single worm using the WGA method is equivalent to using multiple worms. Interestingly, we observed a decrease in reference coverage (97.4% versus 95.8%) and BUSCO completeness (97.6% versus 95.2%) as the number of worms increased from a single worm to 10 worms prior to MDA. In addition, more contaminant sequences were present (14.4–16.9 Mb versus 0.1–0.2 Mb in a single worm) (Supplementary Table S9).

Table 1. Statistics of *C. elegans* genome assemblies

	Reference	Amplified	Unamplified
Reads N50 (kb)	–	7.7	21.1
Depth	–	73.5	88.6
Size (Mb)	100.3	98.4	103.2
Sequence number	7	499	55
Longest (Mb)	20.9	2.7	15.1
Minimum (bp)	13,794	1,447	1,437
N50 (kb)	17,494	656.2	6,868.7
L50	3	43	5
N90 (kb)	13,784	122.0	2,966.0
L90	6	185	13
BUSCO completeness (%) (nematode lineage)	98.8	97.6	98.8
Assembly covered (%)	–	97.4	100.0

High quality annotations from a single nematode genome and transcriptome

To quantify the difference between annotation based on a single worm genome and transcriptome, we profiled the transcriptome from a single *C. elegans* adult based on the Smartseq2 protocol and generated ∼10 Gb of Illumina reads [(48); Supplementary Table S2]. We generated annotations either by *de novo* assembly of these reads or by mapping these reads to the genome assembly and used these reads as evidence in the BRAKER2 pipeline. To evaluate the accuracy of the annotations from different approaches and datasets, all gene predictions were aligned back to the *C. elegans* reference and compared with the most recent annotation of 19,981 protein-encoding genes from WormBase [ver WBPS18; (52)] (Figure 2; Supplementary Table S11). Comparing two versions of the *C.elegans* reference (WBPS18 versus WS100), more loci (19,406 versus 17,153) were annotated in the current reference, demonstrating the improvement in gene annotation over time. Gene structures predicted using single-worm RNA-seq mapped to the reference genome by Stringtie (72) had lower sensitivity and precision compared with the reference proteome, and the BRAKER2 pipeline produced a more accurate prediction when using these mappings as hints. More importantly, the same pipeline produced predictions with only a slightly reduced accuracy of 1.5% on average when the genome-amplified assembly was used instead (Figure 2A). As expected, these annotations were more sensitive and accurate than those that were originally published (WS100) and *de novo* transcriptomes for all metrics (Supplementary

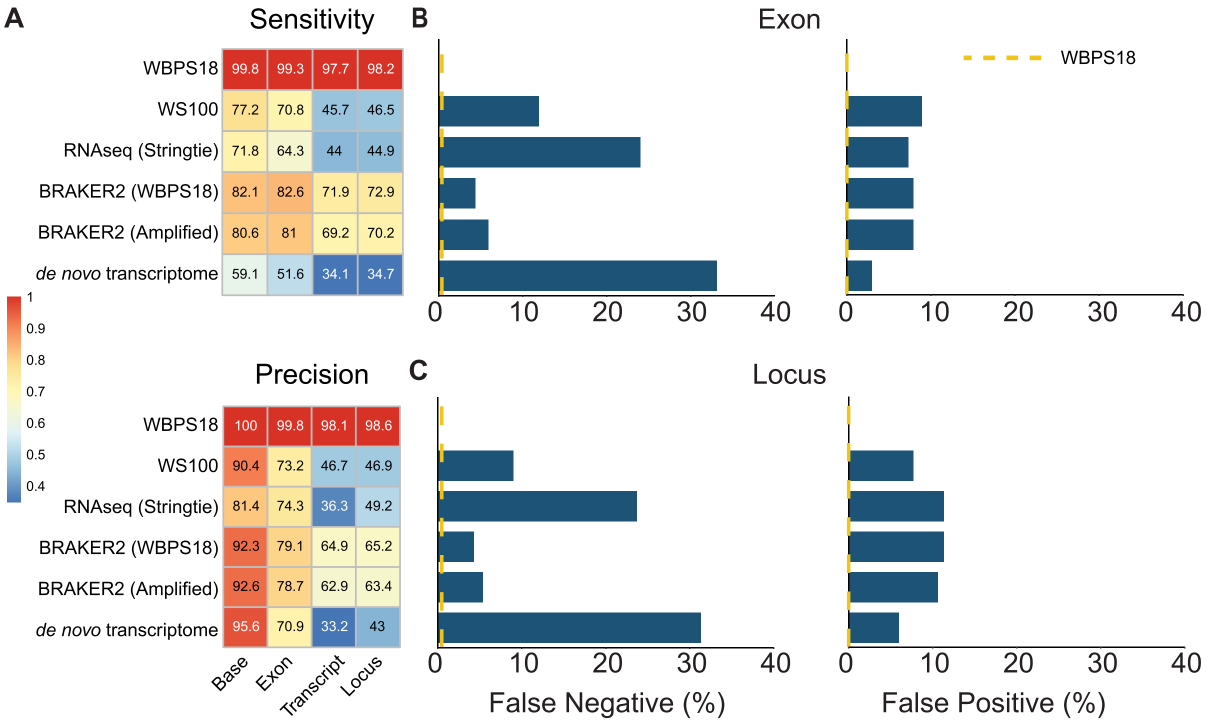

Figure 2. Comparison of annotations using different approaches and datasets. (**A**) Sensitivity and precision on the base, exon, transcript and locus level. WBPS18 indicates the baseline performance when the reference proteome of *C. elegans* was aligned back to its reference genome using Minimap2. The color of the heatmap is the value of each sample divided by the values in the WBPS18 comparison. (**B** and **C**) Percentage of false negatives and false positives in the exon and locus. False negatives are the precentage of reference genes missing from the predictions, whereas false positives are new genes in the predictions that are not present in the reference proteome. A yellow dashed line represents the value of the WBPS18 comparison as baseline.

Table S11). The *de novo* transcriptome had more missing exons (33.1% versus 4.4–24.0%), missing loci (31.3% versus 4.3–23.7%) and fewer matching transcripts (6,821 versus 8,797–14,366) (Figure 2B, C). Of particular note, the proportions of 50% and 95% assembled genes, which are imperative for phylogenomic analyses, were 68.0% and 51.4% lower in the *de novo* transcriptome compared with the annotation produced with the available genome-amplified assembly (Supplementary Table S11). These results indicate that the genome-amplified assemblies can be annotated with reasonable accuracy using the existing pipeline.

Genome characteristics of free-living nemtodes

We applied our optimised sequencing and annotation protocol to 13 free-living nematode genomes from three clades collected from the north coast of Taiwan (Table 2). On average, 12 Gb of palindrome-corrected (Supplementary Figure S6B) ONT genomic reads and 5 Gb of transcriptome reads were sequenced from single adults with a total of two worms per species (Supplementary Table S2) and the genome assemblies ranged from 136.6 to 738.8 Mb. The Chromadoria and Enoplia nematodes have typically larger genome sizes than other clades (Figure 3A), with the *T. latispiculum* 738.8 Mb assembly being the second largest currently recorded in nematodes following the 2.5Gb of the horse parasite *Parascaris univalens* (73). Some of the assemblies may underestimate the true genome size, as the sequence coverage was as low as 11×, warranting additional sequencing. Using the BRAKER2 pipeline, 18,082–35,701 protein-coding genes were annotated in 13 free-living nematode genomes and were 32.6–99.2% complete based on BUSCO analysis (Supplementary Table S12). A positive correlation was observed between the BUSCO score and both genome N50 (Kendall's $\tau = 0.49$, $P = 0.01$) and ONT coverage (Kendall's $\tau = 0.44$, $P = 0.02$). The intron distribution of the Dorylaimia and Chromadoria lineages sequenced in this study had a similar pattern, peaking around 55 bp (Table 2; Supplementary Figure S9), and were similar to previously published nematodes in these clades (74). Interestingly, there are fewer but longer introns in the four Enoplia species, suggesting a different intron distribution in the last common ancestor of this clade compared with the rest of the nematodes (Figure 3B; Supplementary Figure S10). Orthology inference using Orthofinder (57) placed these gene models and those of 13 other nematode genomes into 46,158 orthologous groups. Within these orthologous groups, 50.8% (23,469 orthologous groups) were shared between two or more species, consistent with previous observations of extensive clade-specific families in nematode lineages (75). In addition, 23.6–49.8% of the genes in 13 free-living nematode species were species specific (Supplementary Table S13). The proportion of these species-specific genes was positively correlated with the number of gene models (Kendall's $\tau = 0.7$, $P < 0.001$) but not genome size, assembly N50 or ONT coverage.

Of the 13 nematode species sequenced in this study, nine were able to assemble a circular mitochondrial genome

Table 2. Genome statistics of 13 free-living nematode genome assemblies

Species	Clade	Size (Mb)	Sequence (*n*)	Longest (kb)	N50 (kb)	Gene (*n*)	Intron length median (bp)
Mesodorylaimus sp.	I	142.5	1,557	2,535.9	441	22,631	65
Trissonchulus sp.	II	421.5	17,985	425.7	51.9	35,701	559
T. ribeirensis	II	738.8	30,949	369.1	44.3	18,082	1,893
E. lenunculus	II	286.5	2,646	2,205.1	266.9	24,757	612
T. latispiculum	II	642.2	28,528	427.8	51	26,621	558
Theristus sp.	C	150	4,198	376.4	81.9	18,733	264
S. punctata	C	302.3	7,416	842.6	125.2	29,890	112
Ptycholaimellus sp.	C	219.7	12,974	357.8	37.1	29,037	58
Linhomoeus sp.	C	207.3	13,199	327.6	31.6	28,535	99
Paralinhomoeus sp.	C	147	3,410	697.5	104	24,020	79
Microlaimidae sp.	C	540.3	32,219	243.1	26.3	27,483	1,099
Epsilonema sp.	C	136.6	5,280	530.5	68.2	21,223	264
Rhynchonema sp.	C	205	7,081	692.2	77.6	24,838	231

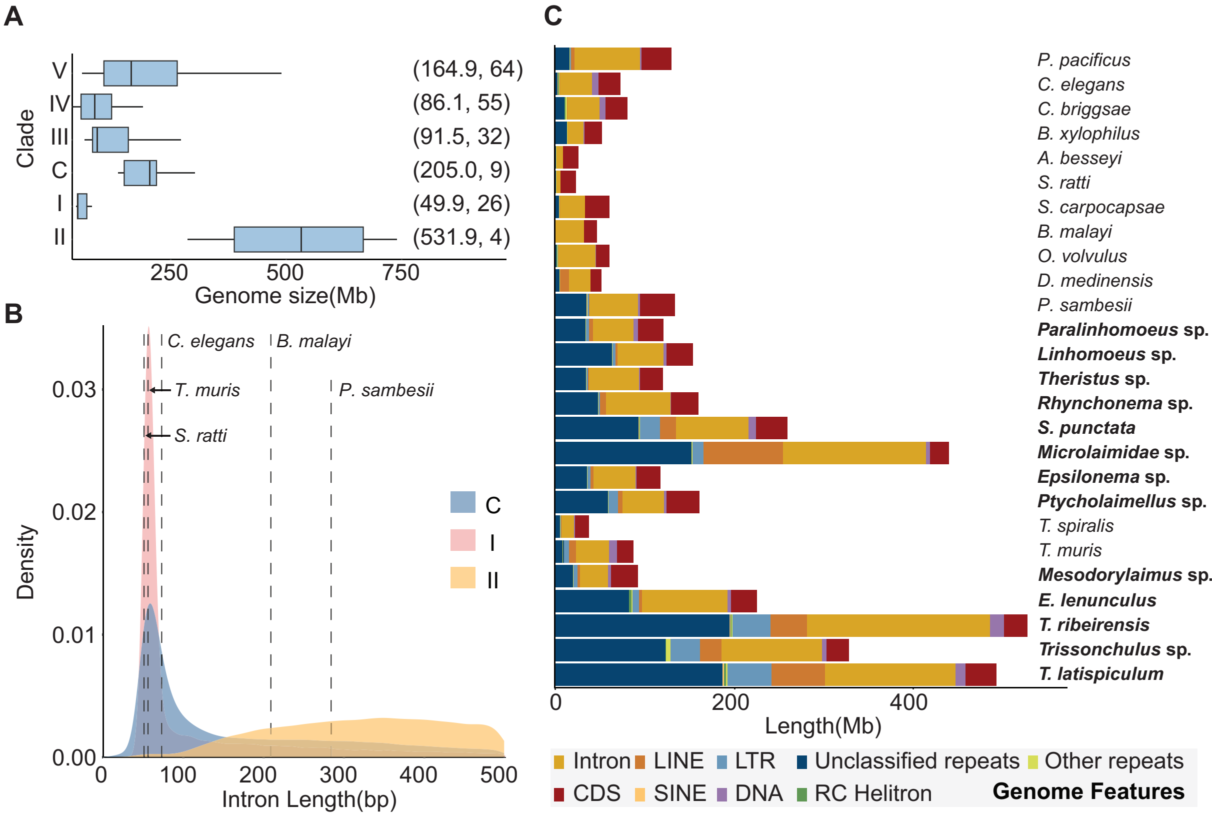

Figure 3. Nematode genome size, intron distribution and genome structure. (**A**) Genome size variation between different nematode clades. The text in parentheses denotes the median genome size in megabases and the number of nematode genomes downloaded from WormBase ParaSite (52) to be included in the analysis, respectively. (**B**) Intron distribution of nematodes. Dashed lines are the intron median of the representative species in clades I, III, IV and V and Chromadoria (C). (**C**) The proportion of different genome features in the nematode genomes. Bold letters represent the nematode genomes assembled in this study. The 'Other repeats' feature includes the sum of tRNA, snRNA, rRNA, simple repeats and satellites.

(mitogenome) with a read coverage depth of 39–2,656×. Interestingly, the 12 proteins typically found in nematode mitogenomes were only completely predicted in five species. These mitogenomes are highly rearranged compared with other clades (Rhabditina, Spirurina and Tylenchina) (Supplementary Figure S11). The gene order in *Mesodorylaimus* sp. showed lack of synteny compared with other species in Dorylaimia, consistent with previous observations of a high rearrangement rate in the Dorylaimia species (76).

The basal Chromadoria and Enoplia assemblies contained significantly more repeats (23.4–50.6%) than the representative nematodes across the other four clades (0.8–31.4%; Figure 3C; Supplementary Figure S12). This is consistent with the previous finding of a marked decrease of transposable element load at ancestral nodes especially at the base of clade III + IV + V (77). In contrast to most published genomes in the Dorylaimia and Rhabditina clades, which were enriched in DNA transposons (75), (Supplementary Figure S13A), LTRs or LINE repeats were more abundant in six free-living nematode species and *T. muris*, especially in the two *Trissonchulus* species (LTRs 7.9% versus 0.1–7.6% in other species). A total of 16,046 unknown repeat families were identified in the 13 nematodes, which were clustered into 16,044 sequence groups based on 90% identity, suggesting that they were species specific. These unclassfied repeats were evenly distributed across the genome with the exception of three species in Enoplia (*Trissonchulus* sp., *T. latispiculum* and *T. ribeirensis*), which each had a dominant family comprising 2.2–5.6% and 0.7–1.5% of the unclassified repeats and genomes, respectively.

Enoplia is sister to the rest of the nematode classes

To support the basal branch order of the Nematoda phylogeny, in particular the relative placement of Enoplia and Dorylaimia, a species tree was inferred based on a coalescent-based analysis (60,78) of 9,343 paralogous gene trees from 26 representative nematode species, and the cactus worm *Priapulus cauatus* as an outgroup. The species phylogeny separated nematodes into six groups, comprising five clades and groups of the early derived Chromadoria lineage (20), and placed Enoplia as a sister group to Dorylaimia and the Chromadoria lineage, both with strong boostrap support (Supplementary Figure S14). The topology remained similar when we included an additional 17 *de novo* transcriptomes from Enoplia and Chromadoria and a further three outgroups (Figure 4) (19,32). The combined phylogeny shows that nematodes can be separated into the previously designated five clades (20) and support for the placement of Enoplia remained robust (Astro-pro, bs = 100). In the early derived Chromadoria lineages, most of the lineages were grouped by order, with the exception of the Monhysterida lineage which was paraphyletic (32).

DISCUSSION

In this study, we demonstrated the feasibility of generating genome assemblies from single adult nematodes using MDA. By testing the protocols on *C. elegans,* we were able to fully quantify the extent of bias and address it with existing analysis pipelines. We demonstrate that a genome assembly and accurate gene annotations can be achieved with this workflow and further sequenced the genomes of 13 free-living nematodes. With a genome size of 136.6–738.8 Mb in 13 nematodes, sequencing on a single MinION flowcell can be expected to provide ∼37.8× depth of coverage. Of these genomes, four are the first reported in the Enoplia clade, revealing their unusually large genome sizes and structures (Figure 3). Through phylogenomics, we established Enoplia as sister to the phylum Nematoda, supporting a marine origin in the last common ancestor of nematodes (19,32). Analysis of repetitive content in these new genomes revealed that transposable element and genome reduction might have taken place in the last common ancestor of clade III + IV + V (77). We bypassed the challenging stage of obtaining axenic cultures (8), whilst assembly and annotation can be achieved within a week of nematode isolation. Assuming that 1 μg is required for long-read sequencing, combining MDA with ONT sequencing thus provides a cost- and labor-effective solution (1) to generate complete assemblies in organisms with as little as 50 pg of starting material. We note that the amplified products no longer contain the native information present on the original templates, such as methylation, which was accessible by single-molecule sequencing. Nevertheless, there is tremendous interest in using the integrated approach to sequence parasitic nematodes (79), different species and sequencing platforms, and at a single-cell resolution (36,80). For example, assembly from PacBio HiFi sequencing of an amplified single human CD8+ T cell resulted in an assembly with 12.8% complete gene models (81).

The advantage of using a single individual for whole-genome sequencing is also seen in the sequencing of organisms such as obligate symbionts and helminth eggs, where it is possible to overcome obstacles such as inability to culture and inaccessibility in the live host (9,82). The use of a single nematode had several benefits over pooling multiple worms, for instance closely related nematode species have imperceptible morphological differences that increased the risk of mixing different species (83,84). For example, a host can be infected with multiple *Anisakis* species with no morphological differences (85). In addition, natural populations are likely to have high levels of heterozygosity, which also affects the quality of assembly and annotation, as observed in this study.

The MDA method used in this study is known to result in uneven read coverage (86). This unevenness is thought to be caused by the formation of secondary structures that reduce the efficiency of the phi29 polymerase used in the amplification process, particularly in repetitive sequences that are prone to forming such structures (63,86). Despite these challenges, only 0.4% of the *C. elegans* genome remained unsequenced including 10 genes. This approach allowed us to effectively assemble the genome, with only 2.5% missing due to the combined challenges posed by repetitive sequences and reduced coverage. A notable limitation is that the N50 of the amplified data appears to be capped at ∼8 kb, with longer reads probably originating from chimeric sequences. This has led to a more fragmented assembly compared with an assembly from an unamplified sample. Nevertheless, the longest non-palindromic sequences ranged from 49.2 to 734.4 kb, demonstrating MDA's capability to amplify long templates. The BUSCO completeness values suggest that the amplified assembly is complete and capable of generating high-quality annotation compared with the reference genome (96.1% versus 98%).

Our study shows that gene predictions from genomes with RNA-seq data as hints outperform *de novo* transcriptome assemblies, especially in the number of 95% assembled loci (84.7% versus 43.1%). This is expected, and a balance needs to be struck between the accuracy of gene prediction per species and the breadth of species sampling. Hence, we advocate for the inclusion of complete assemblies in selected samples to facilitate future phylogenomic analyses initially intended to use only *de novo* transcriptome samples. While the assemblies may not necessarily need to meet reference standards, a caveat is the dependency of predicted gene model accuracy on the quality of assembly consensus and contiguity (87). The latter had a greater impact in our dataset, as indicated by the stronger positive correlation between the BUSCO completeness and assembly N50 over ONT coverage. In addition, the combination of a

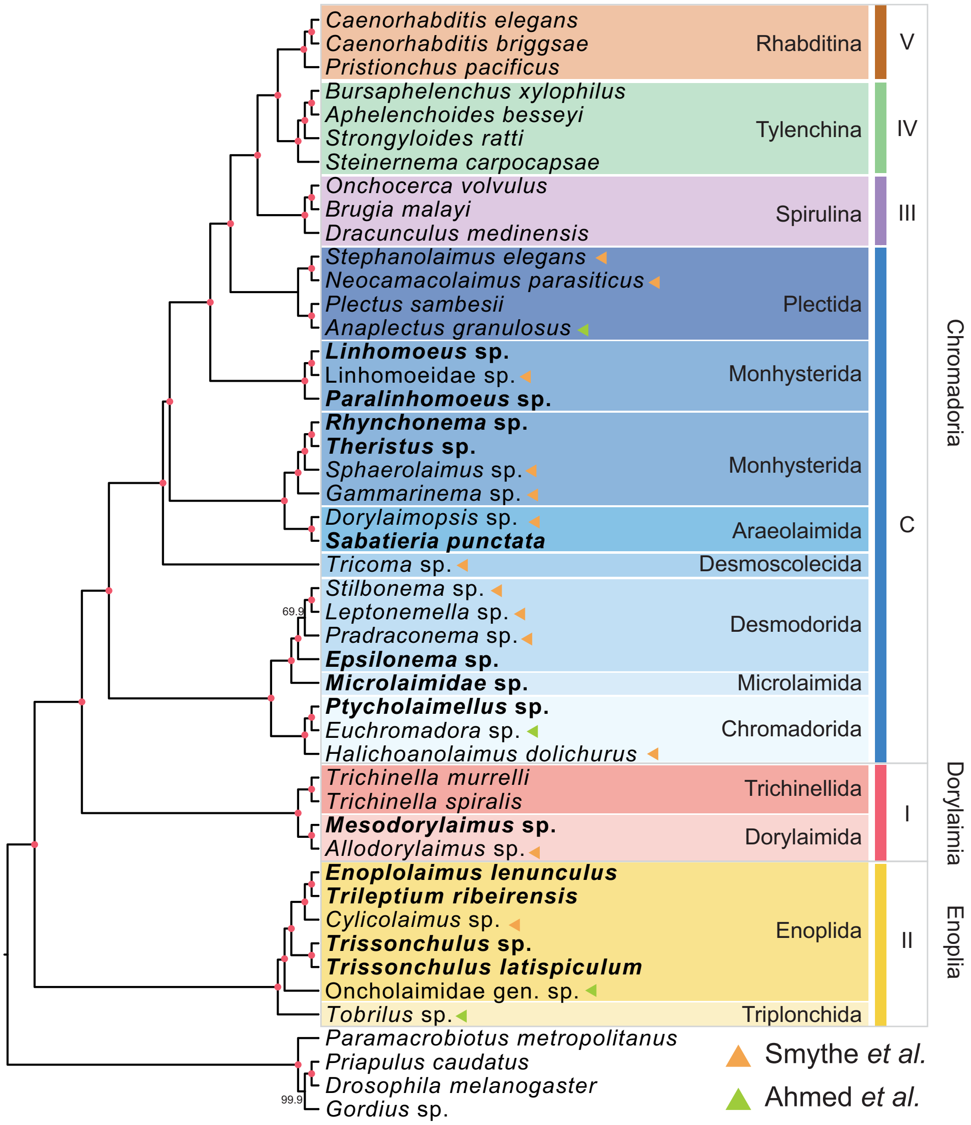

Figure 4. Phylogenetic analysis combining the nematode transcriptome and genome. Bold font represents the genomes sequenced in this study. Roman numerals on the right represent the five clades of Nematoda, and C represents the basal Chromadoria lineage. The colors of triangles denote the data source. The red dots in branches denote a bootstrap support value of 100.

high proportion of species-specific genes coupled with lower BUSCO completeness in some assemblies suggests the presence of mispredictions. A well-known example was the first published *Heterorhabditis bacteriophora* assembly, in which 52.7% of 21,250 gene models had no *C. elegans* homolog and a BUSCO completeness of 47.8% (88). A later improved set of gene models exhibited a 94.0% BUSCO completeness with relatively fewer species-specific genes (89). Despite the presence of potential mispredictions in our dataset, they should not hinder phylogenomic analyses as species-wide orthologs were employed. Supplementing lower coverage assemblies with additional sequencing is likely to improve the overall data quality and result accuracy.

To conclude, we demonstrate the feasibility of incorporatng WGA into investigation of microbial biodiversity from sampling to comparative genomic analysis. By thoroughly characterising and accounting for the inherent limitations of this approach, complete assemblies and accurate gene predictions can be generated. The availability of the new free-living genomes has allowed us to address outstanding questions and offer new biological insights. As long-read sequencing advances in accuracy and affordability, we envisage that a complete assembly will be available for any species that were once considered inaccessible.

DATA AVAILABILITY

All sequences generated from this study were deposited on the NCBI under BioProject PRJNA953805, and the Biosample accession number of the free-living nematodes can be found in Supplementary Table S3. The assemblies and annotations of the 13 free-living species are also available in the WormBase ParaSite ftp (https://ftp.ebi.ac.uk/pub/databases/wormbase/parasite/datasets/PRJNA953805/). The scripts and proteome data are available in Github page: https://yichienlee1010.github.io/Single-nematode-genome/ (permanent doi: https://zenodo.org/record/8144614).

SUPPLEMENTARY DATA

Supplementary Data are available at NAR Online.

ACKNOWLEDGEMENTS

We thank Wei-An Liu for testing out the initial MDA protocols in yeast. We thank the NGS Genomics core lab of Academia Sinica of Taiwan for sequencing the initial single-worm RNA-seq data. We would like to thank the National Center for High-performance Computing (NCHC) of the National Applied Research Laboratories (NARLabs) of Taiwan for providing computational resources and storage resources. We thank Dionysis Grigoriadis for his assistance in uploading the genome assemblies and annotations to the WormBase ParaSite database.

Authors' contributions: I.J.T. conceived the study; Yi.C.L., Yu.C.L., M.C.W. and Y.C.T. carried out the sampling; Yi.C.L. isolated the nematodes; Yi.C.L. and H.M.K. conducted the experiments and ONT sequencing; Yi.C.L. performed the assemblies and annotations with help from H.H.L. and Yu.C.L.; Yi.C.L. carried out analyses. Yi.C.L. and I.J.T. wrote the manuscript with input from T.K. and others. All authors read and approved the final manuscript.

FUNDING

Academia Sinica [AS-CDA-107-L01 to I.J.T.]; the National Science and Technology Council [111-2628-B-001-021 to I.J.T.]; and Taiwan International Graduate Program, Academia Sinica of Taiwan, [doctorate fellowship to Yi.C.L.].

Conflict of interest statement. None declared.

REFERENCES

1. Faulk,C. (2023) De novo sequencing, diploid assembly, and annotation of the black carpenter ant, *Camponotus pennsylvanicus*, and its symbionts by one person for $1000, using nanopore sequencing. *Nucleic Acids Res.*, **51**, 17–28.
2. He,K., Minias,P. and Dunn,P.O. (2021) Long-read genome assemblies reveal extraordinary variation in the number and structure of MHC loci in birds. *Genome Biol. Evol.*, **13**, evaa270.
3. Rhie,A., McCarthy,S.A., Fedrigo,O., Damas,J., Formenti,G., Koren,S., Uliano-Silva,M., Chow,W., Fungtammasan,A., Kim,J. *et al.* (2021) Towards complete and error-free genome assemblies of all vertebrate species. *Nature*, **592**, 737–746.
4. Hotaling,S., Sproul,J.S., Heckenhauer,J., Powell,A., Larracuente,A.M., Pauls,S.U., Kelley,J.L. and Frandsen,P.B. (2021) Long reads are revolutionizing 20 years of insect genome sequencing. *Genome Biol. Evol.*, **13**, evab138.
5. Runnel,K., Abarenkov,K., Copot,O., Mikryukov,V., Koljalg,U., Saar,I. and Tedersoo,L. (2022) DNA barcoding of fungal specimens using PacBio long-read high-throughput sequencing. *Mol. Ecol. Resour.*, **22**, 2871–2879.
6. Lewin,H.A., Richards,S., Lieberman Aiden,E., Allende,M.L., Archibald,J.M., Balint,M., Barker,K.B., Baumgartner,B., Belov,K., Bertorelle,G. *et al.* (2022) The Earth BioGenome Project 2020: starting the clock. *Proc. Natl Acad. Sci. USA*, **119**, e2115635118.
7. Ekblom,R. and Galindo,J. (2011) Applications of next generation sequencing in molecular ecology of non-model organisms. *Heredity (Edinb.)*, **107**, 1–15.
8. Hongoh,Y. and Toyoda,A. (2011) Whole-genome sequencing of unculturable bacterium using whole-genome amplification. *Methods Mol. Biol.*, **733**, 25–33.
9. Montoliu-Nerin,M., Sanchez-Garcia,M., Bergin,C., Grabherr,M., Ellis,B., Kutschera,V.E., Kierczak,M., Johannesson,H. and Rosling,A. (2020) Building de novo reference genome assemblies of complex eukaryotic microorganisms from single nuclei. *Sci. Rep.*, **10**, 1303.
10. Deleye,L., Tilleman,L., Vander Plaetsen,A.S., Cornelis,S., Deforce,D. and Van Nieuwerburgh,F. (2017) Performance of four modern whole genome amplification methods for copy number variant detection in single cells. *Sci. Rep.*, **7**, 3422.
11. Santoro,A.E., Kellom,M. and Laperriere,S.M. (2019) Contributions of single-cell genomics to our understanding of planktonic marine archaea. *Philos. Trans. R Soc. B Biol. Sci.*, **374**, 20190096.
12. Sahraei,S.E., Sanchez-Garcia,M., Montoliu-Nerin,M., Manyara,D., Bergin,C., Rosendahl,S. and Rosling,A. (2022) Whole genome analyses based on single, field collected spores of the arbuscular mycorrhizal fungus *Funneliformis geosporum*. *Mycorrhiza*, **32**, 361–371.
13. Lepere,C., Demura,M., Kawachi,M., Romac,S., Probert,I. and Vaulot,D. (2011) Whole-genome amplification (WGA) of marine photosynthetic eukaryote populations. *FEMS Microbiol. Ecol.*, **76**, 513–523.
14. Nyaku,S.T., Sripathi,V.R., Lawrence,K. and Sharma,G. (2021) Characterizing repeats in two whole-genome amplification methods in the reniform nematode genome. *Int. J. Genomics.*, **2021**, 5532885.
15. Eccles,D., Chandler,J., Camberis,M., Henrissat,B., Koren,S., Le Gros,G. and Ewbank,J.J. (2018) De novo assembly of the complex genome of *Nippostrongylus brasiliensis* using MinION long reads. *BMC Biol.*, **16**, 6.
16. Dillman,A.R., Mortazavi,A. and Sternberg,P.W. (2012) Incorporating genomics into the toolkit of nematology. *J. Nematol.*, **44**, 191–205.
17. Dieterich,C. and Sommer,R.J. (2009) How to become a parasite—lessons from the genomes of nematodes. *Trends Genet.*, **25**, 203–209.
18. Larsen,B.B., Miller,E.C., Rhodes,M.K. and Wiens,J.J. (2017) Inordinate fondness multiplied and redistributed: the number of species on Earth and the new pie of life. *Q. Rev. Biol.*, **92**, 229–265.
19. Smythe,A.B., Holovachov,O. and Kocot,K.M. (2019) Improved phylogenomic sampling of free-living nematodes enhances resolution of higher-level nematode phylogeny. *BMC Evol. Biol.*, **19**, 121.
20. Blaxter,M.L., De Ley,P., Garey,J.R., Liu,L.X., Scheldeman,P., Vierstraete,A., Vanfleteren,J.R., Mackey,L.Y., Dorris,M., Frisse,L.M. *et al.* (1998) A molecular evolutionary framework for the phylum Nematoda. *Nature*, **392**, 71–75.
21. De Ley,P. (2006) A quick tour of nematode diversity and the backbone of nematode phylogeny. *WormBook*, 1–8.
22. Kern,E.M.A., Kim,T. and Park,J.K. (2020) The mitochondrial genome in nematode phylogenetics. *Front. Ecol. Evol.*, **8**, https://doi.org/10.3389/fevo.2020.00250.
23. The *C. elegans* Sequencing Consortium. (1998) Genome sequence of the nematode *C. elegans*: a platform for investigating biology. *Science*, **282**, 2012–2018.
24. Kikuchi,T., Eves-van den Akker,S. and Jones,J.T. (2017) Genome evolution of plant-parasitic nematodes. *Annu. Rev. Phytopathol.*, **55**, 333–354.
25. Mahfouz,M.M. and Abd-Elgawad,T.H.A. (2015) In: *Impact of Phytonematodes on Agriculture Economy*. CAB International, Wallingford, UK.
26. Xie,Y., Zhang,P., Xue,B., Cao,X., Ren,X., Wang,L., Sun,Y., Yang,H. and Zhang,L. (2020) Establishment of a marine nematode model for animal functional genomics, environmental adaptation and developmental evolution. bioRxiv doi: https://doi.org/10.1101/2020.03.06.980219, 07 March 2020, preprint: not peer reviewed.
27. Gingold,R., Moens,T. and Rocha-Olivares,A. (2013) Assessing the response of nematode communities to climate change-driven warming: a microcosm experiment. *PLoS One*, **8**, e66653.
28. Moens,T. and Vincx,M. (2000) Temperature, salinity and food thresholds in two brackish-water bacterivorous nematode species: assessing niches from food absorption and respiration experiments. *J. Exp. Mar. Biol. Ecol.*, **243**, 137–154.
29. Viney,M. (2017) How can we understand the genomic basis of nematode parasitism? *Trends Parasitol.*, **33**, 444–452.

30. Meldal,B.H., Debenham,N.J., De Ley,P., De Ley,I.T., Vanfleteren,J.R., Vierstraete,A.R., Bert,W., Borgonie,G., Moens,T., Tyler,P.A. *et al.* (2007) An improved molecular phylogeny of the Nematoda with special emphasis on marine taxa. *Mol. Phylogenet. Evol.*, **42**, 622–636.
31. Bik,H.M., Lambshead,P.J., Thomas,W.K. and Lunt,D.H. (2010) Moving towards a complete molecular framework of the Nematoda: a focus on the Enoplida and early-branching clades. *BMC Evol. Biol.*, **10**, 353.
32. Ahmed,M., Roberts,N.G., Adediran,F., Smythe,A.B., Kocot,K.M. and Holovachov,O. (2022) Phylogenomic analysis of the phylum nematoda: conflicts and congruences with morphology, 18S rRNA, and mitogenomes. *Front Ecol. Evol.*, **9**, https://doi.org/10.3389/fevo.2021.769565.
33. Marcais,G. and Kingsford,C. (2011) A fast, lock-free approach for efficient parallel counting of occurrences of k-mers. *Bioinformatics*, **27**, 764–770.
34. Ranallo-Benavidez,T.R., Jaron,K.S. and Schatz,M.C. (2020) GenomeScope 2.0 and Smudgeplot for reference-free profiling of polyploid genomes. *Nat. Commun.*, **11**, 1432.
35. Li,H. (2018) Minimap2: pairwise alignment for nucleotide sequences. *Bioinformatics*, **34**, 3094–3100.
36. Warris,S., Schijlen,E., van de Geest,H., Vegesna,R., Hesselink,T., Te Lintel Hekkert,B., Sanchez Perez,G., Medvedev,P., Makova,K.D. and de Ridder,D. (2018) Correcting palindromes in long reads after whole-genome amplification. *BMC Genomics*, **19**, 798.
37. Kolmogorov,M., Yuan,J., Lin,Y. and Pevzner,P.A. (2019) Assembly of long, error-prone reads using repeat graphs. *Nat. Biotechnol.*, **37**, 540–546.
38. Vaser,R., Sovic,I., Nagarajan,N. and Sikic,M. (2017) Fast and accurate de novo genome assembly from long uncorrected reads. *Genome Res.*, **27**, 737–746.
39. Hu,J., Fan,J., Sun,Z. and Liu,S. (2020) NextPolish: a fast and efficient genome polishing tool for long-read assembly. *Bioinformatics*, **36**, 2253–2255.
40. Huang,S., Kang,M. and Xu,A. (2017) HaploMerger2: rebuilding both haploid sub-assemblies from high-heterozygosity diploid genome assembly. *Bioinformatics*, **33**, 2577–2579.
41. Simao,F.A., Waterhouse,R.M., Ioannidis,P., Kriventseva,E.V. and Zdobnov,E.M. (2015) BUSCO: assessing genome assembly and annotation completeness with single-copy orthologs. *Bioinformatics*, **31**, 3210–3212.
42. Quinlan,A.R. and Hall,I.M. (2010) BEDTools: a flexible suite of utilities for comparing genomic features. *Bioinformatics*, **26**, 841–842.
43. Bankevich,A., Nurk,S., Antipov,D., Gurevich,A.A., Dvorkin,M., Kulikov,A.S., Lesin,V.M., Nikolenko,S.I., Pham,S., Prjibelski,A.D. *et al.* (2012) SPAdes: a new genome assembly algorithm and its applications to single-cell sequencing. *J. Comput. Biol.*, **19**, 455–477.
44. Buchfink,B., Reuter,K. and Drost,H.-G. (2021) Sensitive protein alignments at tree-of-life scale using DIAMOND. *Nat. Methods*, **18**, 366–368.
45. De Vivo,M., Lee,H.-H., Huang,Y.-S., Dreyer,N., Fong,C.-L., de Mattos,F.M.G., Jain,D., Wen,Y.-H.V., Mwihaki,J.K., Wang,T.-Y. *et al.* (2022) Utilisation of Oxford Nanopore sequencing to generate six complete gastropod mitochondrial genomes as part of a biodiversity curriculum. *Sci. Rep.*, **12**, 9973.
46. Bernt,M., Donath,A., Juhling,F., Externbrink,F., Florentz,C., Fritzsch,G., Putz,J., Middendorf,M. and Stadler,P.F. (2013) MITOS: improved de novo metazoan mitochondrial genome annotation. *Mol. Phylogenet. Evol.*, **69**, 313–319.
47. Mikheenko,A., Prjibelski,A., Saveliev,V., Antipov,D. and Gurevich,A. (2018) Versatile genome assembly evaluation with QUAST-LG. *Bioinformatics*, **34**, i142–i150.
48. Serra,L., Chang,D.Z., Macchietto,M., Williams,K., Murad,R., Lu,D., Dillman,A.R. and Mortazavi,A. (2018) Adapting the Smart-seq2 protocol for robust single worm RNA-seq. *Bio. Protoc.*, **8**, e2729.
49. Bolger,A.M., Lohse,M. and Usadel,B. (2014) Trimmomatic: a flexible trimmer for Illumina sequence data. *Bioinformatics*, **30**, 2114–2120.
50. Flynn,J.M., Hubley,R., Goubert,C., Rosen,J., Clark,A.G., Feschotte,C. and Smit,A.F. (2020) RepeatModeler2 for automated genomic discovery of transposable element families. *Proc. Natl Acad. Sci. USA*, **117**, 9451–9457.
51. Edgar,R.C. (2010) Search and clustering orders of magnitude faster than BLAST. *Bioinformatics*, **26**, 2460–2461.
52. Howe,K.L., Bolt,B.J., Shafie,M., Kersey,P. and Berriman,M. (2017) WormBase ParaSite—a comprehensive resource for helminth genomics. *Mol. Biochem. Parasitol.*, **215**, 2–10.
53. Dobin,A. and Gingeras,T.R. (2015) Mapping RNA-seq reads with STAR. *Curr. Protoc. Bioinformatics*, **51**, 11.14.1–11.14.19.
54. Bruna,T., Hoff,K.J., Lomsadze,A., Stanke,M. and Borodovsky,M. (2021) BRAKER2: automatic eukaryotic genome annotation with GeneMark-EP+ and AUGUSTUS supported by a protein database. *NAR Genom. Bioinform.*, **3**, lqaa108.
55. Pertea,G. and Pertea,M. (2020) GFF utilities: gffRead and GffCompare. *F1000Res*, **9**, ISCB Comm J-304.
56. Wood,D.E., Lu,J. and Langmead,B. (2019) Improved metagenomic analysis with Kraken 2. *Genome Biol.*, **20**, 257.
57. Emms,D.M. and Kelly,S. (2015) OrthoFinder: solving fundamental biases in whole genome comparisons dramatically improves orthogroup inference accuracy. *Genome Biol.*, **16**, 157.
58. Katoh,K. and Standley,D.M. (2013) MAFFT multiple sequence alignment software version 7: improvements in performance and usability. *Mol. Biol. Evol.*, **30**, 772–780.
59. Piñeiro,C., Abuín,J.M. and Pichel,J.C. (2020) Very Fast Tree: speeding up the estimation of phylogenies for large alignments through parallelization and vectorization strategies. *Bioinformatics*, **36**, 4658–4659.
60. Zhang,C., Scornavacca,C., Molloy,E.K. and Mirarab,S. (2020) ASTRAL-Pro: quartet-based species-tree inference despite paralogy. *Mol. Biol. Evol.*, **37**, 3292–3307.
61. Carlton,P.M., Davis,R.E. and Ahmed,S. (2022) Nematode chromosomes. *Genetics*, **221**, iyac014.
62. Blainey,P.C. and Quake,S.R. (2011) Digital MDA for enumeration of total nucleic acid contamination. *Nucleic Acids Res.*, **39**, e19.
63. Sidore,A.M., Lan,F., Lim,S.W. and Abate,A.R. (2016) Enhanced sequencing coverage with digital droplet multiple displacement amplification. *Nucleic Acids Res.*, **44**, e66.
64. Kim,S.C., Premasekharan,G., Clark,I.C., Gemeda,H.B., Paris,P.L. and Abate,A.R. (2017) Measurement of copy number variation in single cancer cells using rapid-emulsification digital droplet MDA. *Microsyst. Nanoeng.*, **3**, 17018.
65. Tyson,J.R., O'Neil,N.J., Jain,M., Olsen,H.E., Hieter,P. and Snutch,T.P. (2018) MinION-based long-read sequencing and assembly extends the *Caenorhabditis elegans* reference genome. *Genome Res.*, **28**, 266–274.
66. Lai,C.K., Lee,Y.C., Ke,H.M., Lu,M.R., Liu,W.A., Lee,H.H., Liu,Y.C., Yoshiga,T., Kikuchi,T., Chen,P.J. *et al.* (2023) The Aphelenchoides genomes reveal substantial horizontal gene transfers in the last common ancestor of free-living and major plant-parasitic nematodes. *Mol. Ecol. Resour.*, **23**, 905–919.
67. Arroyo Muhr,L.S., Lagheden,C., Hassan,S.S., Kleppe,S.N., Hultin,E. and Dillner,J. (2020) De novo sequence assembly requires bioinformatic checking of chimeric sequences. *PLoS One*, **15**, e0237455.
68. Lasken,R.S. and Stockwell,T.B. (2007) Mechanism of chimera formation during the Multiple Displacement Amplification reaction. *BMC Biotechnol.*, **7**, 19.
69. Calus,S.T., Ijaz,U.Z. and Pinto,A.J. (2018) NanoAmpli-Seq: a workflow for amplicon sequencing for mixed microbial communities on the nanopore sequencing platform. *Gigascience*, **7**, giy140.
70. Muller,B., Jones,C. and West,S.C. (1990) T7 endonuclease I resolves Holliday junctions formed in vitro by RecA protein. *Nucleic Acids Res.*, **18**, 5633–5636.
71. Yoshimura,J., Ichikawa,K., Shoura,M.J., Artiles,K.L., Gabdank,I., Wahba,L., Smith,C.L., Edgley,M.L., Rougvie,A.E., Fire,A.Z. *et al.* (2019) Recompleting the *Caenorhabditis elegans* genome. *Genome Res.*, **29**, 1009–1022.
72. Pertea,M., Pertea,G.M., Antonescu,C.M., Chang,T.C., Mendell,J.T. and Salzberg,S.L. (2015) StringTie enables improved reconstruction of a transcriptome from RNA-seq reads. *Nat. Biotechnol.*, **33**, 290–295.
73. Wang,J., Gao,S., Mostovoy,Y., Kang,Y., Zagoskin,M., Sun,Y., Zhang,B., White,L.K., Easton,A., Nutman,T.B. *et al.* (2017) Comparative genome analysis of programmed DNA elimination in nematodes. *Genome Res.*, **27**, 2001–2014.

74. Ma,M.Y., Xia,J., Shu,K.X. and Niu,D.K. (2022) Intron losses and gains in the nematodes. *Biol. Direct*, **17**, 13.
75. Coghlan,A., Tyagi,R., Cotton,J.A., Holroyd,N., Rosa,B.A., Tsai,I.J., Laetsch,D.R., Beech,R.N., Day,T.A., Hallsworth-Pepin,K. *et al.* (2019) Comparative genomics of the major parasitic worms. *Nat. Genet.*, **51**, 163–174.
76. Hyman,B.C., Lewis,S.C., Tang,S. and Wu,Z. (2011) Rampant gene rearrangement and haplotype hypervariation among nematode mitochondrial genomes. *Genetica*, **139**, 611–615.
77. Szitenberg,A., Cha,S., Opperman,C.H., Bird,D.M., Blaxter,M.L. and Lunt,D.H. (2016) Genetic drift, not life history or RNAi, determine long-term evolution of transposable elements. *Genome Biol. Evol.*, **8**, 2964–2978.
78. Smith,M.L., Vanderpool,D. and Hahn,M.W. (2022) Using all gene families vastly expands data available for phylogenomic inference. *Mol. Biol. Evol.*, **39**, msac112.
79. Stevens,L., Martinez-Ugalde,I., King,E., Wagah,M., Absolon,D., Bancroft,R., de laRosa,P.G., Hall,J.L., Kieninger,M., Kloch,A. *et al.* (2023) Ancient diversity in host–parasite interaction genes in a model parasitic nematode. bioRxiv doi: https://doi.org/10.1101/2023.04.17.535870, 17 April 2023, preprint: not peer reviewed.
80. Kiguchi,Y., Nishijima,S., Kumar,N., Hattori,M. and Suda,W. (2021) Long-read metagenomics of multiple displacement amplified DNA of low-biomass human gut phageomes by SACRA pre-processing chimeric reads. *DNA Res.*, **28**, dsab019.
81. Hård,J., Mold,J.E., Eisfeldt,J., Tellgren-Roth,C., Häggqvist,S., Bunikis,I., Contreras-Lopez,O., Chin,C.-S., Nordlund,J., Rubin,C.-J. *et al.* (2023) Long-read whole genome analysis of human single cells. bioRxiv doi: https://doi.org/10.1101/2021.04.13.439527, 23 January 2023, preprint: not peer reviewed.
82. Doyle,S.R., Sankaranarayanan,G., Allan,F., Berger,D., Jimenez Castro,P.D., Collins,J.B., Crellen,T., Duque-Correa,M.A., Ellis,P., Jaleta,T.G. *et al.* (2019) Evaluation of DNA extraction methods on individual helminth egg and larval stages for whole-genome sequencing. *Front. Genet.*, **10**, 826.
83. Bogale,M., Baniya,A. and DiGennaro,P. (2020) Nematode identification techniques and recent advances. *Plants (Basel)*, **9**, 1260.
84. Subbotin,S.A., Oliveira,C.J., Alvarez-Ortega,S., Desaeger,J.A., Crow,W., Overstreet,C., Leahy,R., Vau,S. and Inserra,R.N. (2021) The taxonomic status of *Aphelenchoides besseyi* Christie, 1942 (Nematoda: aphelenchoididae) populations from the southeastern USA, and description of *Aphelenchoides pseudobesseyi* sp. n. *Nematology*, **23**, 381–413.
85. Van Hien,H., Thi Dung,B., Ngo,H.D. and Doanh,P.N. (2021) First morphological and molecular identification of third-stage larvae of *Anisakis typica* (Nematoda: anisakidae) from marine fishes in Vietnamese water. *J. Nematol.*, **53**, e2021-10.
86. Tsai,I.J., Hunt,M., Holroyd,N., Huckvale,T., Berriman,M. and Kikuchi,T. (2014) Summarizing specific profiles in Illumina sequencing from whole-genome amplified DNA. *DNA Res.*, **21**, 243–254.
87. Denton,J.F., Lugo-Martinez,J., Tucker,A.E., Schrider,D.R., Warren,W.C. and Hahn,M.W. (2014) Extensive error in the number of genes inferred from draft genome assemblies. *PLoS Comput. Biol.*, **10**, e1003998.
88. Bai,X., Adams,B.J., Ciche,T.A., Clifton,S., Gaugler,R., Kim,K.S., Spieth,J., Sternberg,P.W., Wilson,R.K. and Grewal,P.S. (2013) A lover and a fighter: the genome sequence of an entomopathogenic nematode *Heterorhabditis bacteriophora*. *PLoS One*, **8**, e69618.
89. McLean,F., Berger,D., Laetsch,D.R., Schwartz,H.T. and Blaxter,M. (2018) Improving the annotation of the *Heterorhabditis bacteriophora* genome. *Gigascience*, **7**, giy034.